Research Article

Crystal structure and molecular docking studies of benzo[8]annulenes as potential inhibitors against *Mycobacterium tuberculosis*

RA Nagalakshmi[1], J Suresh[1], S Maharani[2] and R Ranjith Kumar[2]

[1]Department of Physics, The Madura College (Autonomous), Madurai, 625 011, India
[2]Department of Organic Chemistry, School of Chemistry, Madurai Kamaraj University, Madurai, 625 021, India

Received on December 23, 2015; Accepted on July 10, 2016; Published on July 31, 2016

Correspondence should be addressed to J Suresh; E-mail: ambujasureshj@yahoo.com

Abstract

Tuberculosis is a disease caused by *Mycobacterium tuberculosis*. The bacterial cell wall has a characteristic low permeability, which essentially makes antibiotics ineffective. The cell wall material must be regulated so that its deposition does not compromise its structure. In this study, two new inhibitors, 2-amino-4-(4-cholorophenyl)-5,6,7,8,9,10-hexahydrobenzo[8] annulene-1,3,3(4H)-tricarbonitrile(Ia) and 2-amino-4-(4-bromophenyl)-5,6,7,8,9,10-hexahydrobenzo[8] annulene-1,3,3(4H)-tricarbonitrile(Ib) were synthesized. The crystal structures of the above compounds were determined by single crystal X-ray diffraction. The compounds C_{21} H_{19} Cl N_3 (Ia) and C_{21} H_{19} Br N_3 (Ib) were crystallized in the monoclinic and triclinic system. In both compounds, the cyclohexane ring was found to adopt a boat conformation. The cyclooctane ring of both compounds adopted a twisted chair-chair conformation**.** *In silico* analyses revealed that both compounds showed good anti-mycobacterial activities against the enoyl-acyl carrier enzyme and the N-acetyl -gamma protein, both of which are critical for bacterial survival. Synthesis, structure determination, conformation, intra, inter-molecular interactions and docking studies of both compounds are presented herein.

Introduction

Tuberculosis (TB) is an infection caused by slow-growing bacteria and remains a leading cause of human suffering and death (Tiruviluamala *et al.* 2002, Smith 2003, Schluger *et al.* 2005). *Mycobacterium tuberculosis* has a unique membrane structure composed largely of lipids that have long-chain fatty acids, called mycolic acids.

The enoyl-acyl carrier protein reductase enzyme (InhA) catalyzes the NADH-dependent reduction of unsaturated, long chain, β-branched fatty acids (mycolic acids), which are essential for bacterial cell wall synthesis. *Mycobacterium tuberculosis* InhA is a fundamental target for anti-tuberculosis intervention (Bradford *et al.* 1998, Dessen *et al.* 1995, Rozwarski *et al.* 1998). Inhibition of the enzyme leads to an increased bacterial vulnerability to external oxidative attacks and ultimately to bacterial death.

The enzyme N-acetyl-gamma-glutamyl-phosphate reductase (AGPR) catalyzes the nicotinamide adenine dinucleotide phosphate (NADPH)-dependent reductive dephosphorylation of N-acetyl-gamma-glutamyl-phosphate to N-acetylglutamate-gamma-semialdehyde. This reaction is the third step in the argentine-biosynthetic pathway (Cybis & Davis 1975) that is essential for some microorganisms and plants, and in particular for *Mycobacterium tuberculo-*

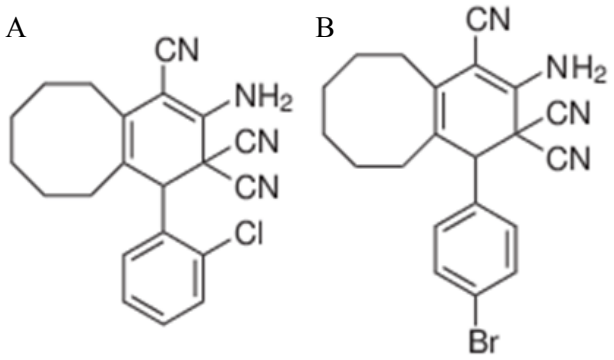

Figure 1. Chemical diagram of the molecule (Ia) (A) and (Ib) (B).

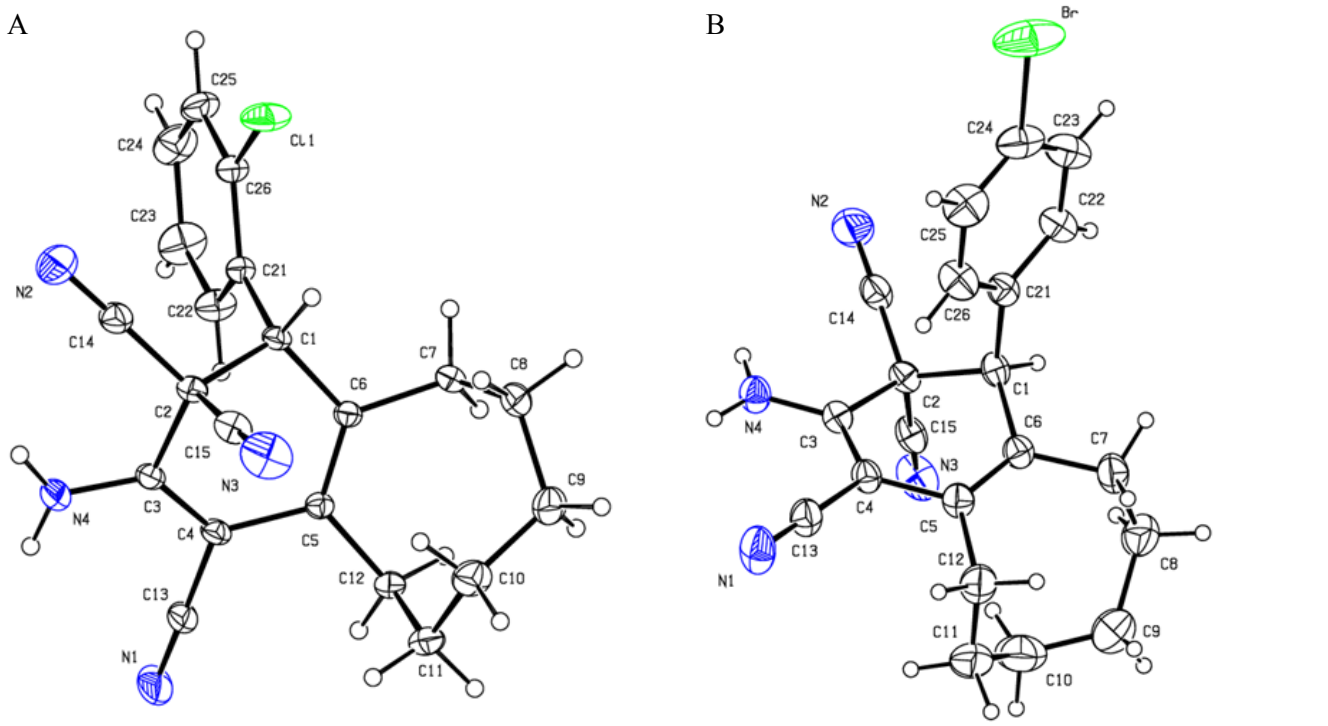

Figure 2. The molecular structure of compounds (Ia**)** (A) and (Ib) (B), showing the atom numbering scheme. Displacement ellipsoids are drawn at 30% probability level, using Platon (Spek 2008).

sis. Inhibition of this protein leads to inhibition of the argentine biosynthesis.

Isoniazid is a narrow spectrum anti-mycobacterial agent. Activated isoniazid causes inhibition of mycolic acid synthesis. A series of 2-benzylsulfanyl derivatives of benzooxazole and benzothiazole have shown their anti-mycobacterial activity against *Mycobacterium tuberculosis* (Koci *et al.* 2002). Sanna *et al.* (2000) synthesized a series of aryl substituted-[1H(2H)benzotriazol-1(2)-yl]acrylnitriles and have also reported anti-mycobacterial activity of the latter. The emergence of multi drug resistant TB (*MDR-TB*) and extensively drug resistance (XDR-TB) makes the treatment ineffective. The drug resistant and HIV co-infection have resulted in the need for new anti -tuberculosis drugs. Continuing our work in developing new drug-like agents for *Mycobacterium tuberculosis* (Nagalakshmi *et.al.* 2014, Suresh *et al.* 2012, Vishnupriya *et al.* 2014), two new benzo[8]annulene compounds were synthesized. The structures of both compounds were studied using single crystal X-ray diffraction. Here we report the synthesis and single crystal X-ray studies of 2-amino-4-(4-cholorophenyl)-5,6,7,8,9,10-hexahydrobenzo[8]annulene-1,3,3(4H)-tricarbonitrile (Ia) and 2-amino-4-(4-bromo phenyl)-5,6,7,8,9,10-hexahydrobenzo[8]annulene-1,3,3(4H)-tricarbonitrile (Ib) (Figure 1) together with docking studies.

Materials and Methods

Preparation of compound (Ia)

A mixture of cyclooctanone (1 mmol), 2-choloro benzaldehyde (1 mmol) and malononitrile (2 mmol) was solvated in ethanol to which NaOEt (0.5 mmol) was added. All chemicals were purchased from Sigma-Aldrich (St. Louis, MO) and were used without further purification. The reaction mixture was heated under reflux for 2–3 hours. As soon as the completion of the reaction was confirmed by thin layer chromatography, the remaining solid mater was filtered and dried. The solid was then crystallized from ethyl acetate, which yielded colorless crystals. The melting point was 470 K and yield was 85%.

Preparation of compound (Ib)

A mixture of cyclooctanone (1 mmol), 4-bromo benzaldehyde (1 mmol) and malononitrile (2 mmol) was taken in ethanol to which NaOEt (0.5 mmol) was added. The reaction mixture was heated under reflux for 2-3 hours. As soon as the completion of the reaction was confirmed by thin layer chromatography, the remaining solid mater was filtered and dried. The solid was then crystallized from ethyl acetate, which yielded colorless crystals. The melting point was 461 K and yield was 85%.

Table 1. The crystal data, intensity data collection and structure solution and structure refinement parameters of compounds **(**Ia) and (Ib).

Empirical formula	C_{21} H_{19} Cl N_4	C_{21} H_{19} Br N_4
Formula weight	362.85	407.31
Temperature	293(2) K	293(2) K
Wavelength	0.71073 Å	0.71073 Å
Crystal system / space group	Monoclinic/ $P2_1/c$	Triclinic/ P-1
Unit cell Dimensions	a = 13.630(11) Å	a = 7.4208(5) Å
	b = 10.475(8) Å	b = 10.160(6) Å
	c = 13.8690(4) Å	c = 13.955(8) Å
	α = 90°	α = 70.635(3)°
	β = 107.403(2)°	β = 77.70(3)°
	γ = 90°	γ = 87.80(3)°
Volume	1889.6(3) Å3	969.35(11) Å3
Z/ Density (calculated)	4/ 1.275 mg/m^3	2/1.395 mg/m^3
Absorption coefficient	0.214 mm^{-1}	2.132 mm^{-1}
F(000)	760	416
Crystal size	0.21x0.19 x0.18 mm^3	0.20 x 0.19 x 0.17 mm^3
Theta range for data collection	2.48 to 30.17°.	2.81 to 25.49°.
Limiting indices	-19<=h<=19, -14<=k<=14, -16<=l<=19	-8<=h<=8, -12<=k<=12, -16<=l<=16
Reflections collected	25664	19116
Independent reflections	5443 [R(int) = 0.0363]	3591 [R(int) = 0.036]
Completeness to theta = 25.50°	99.9 %	99.9 %
Refinement method	Full-matrix least -squares on F^2	Full-matrix least -squares on F^2
Data / restraints / parameters	5443 / 2 / 235	3591 / 1 / 235
Goodness-of-fit on F2	1.025	1.05
Final R indices [I>2sigma(I)]	R1 = 0.0491, wR2 = 0.1068	R1 = 0.0534, wR2 = 0.1252
R indices (all data)	R1 = 0.0898, wR2 = 0.1280	R1 = 0.0926, wR2 = 0.1425
Largest diff. peak and hole	0.214 and -0.303 e.Å-3	0.782 and -1.342 e.Å-3

Structure Determination and Refinement

X-ray diffraction intensity data were collected for compounds (Ia) and (Ib) on the Bruker Smart Apex II single crystal X-ray diffractrometer, equipped with graphite mono-chromated (MoKα) λ=0.7103 Å radiation and CCD detector. Crystals were cut to a suitable size and mounted on a glass fibre using cyanoacrylate adhesive. The unit cell parameters were determined from 36 frames measured (0.5° ω and φ scans) from three different crystallographic zones, using the method of difference vectors. The intensity data collection, frames integration, Lorentz-Polarization correction and decay correction were performed using *SAINT* (Bruker 2004). Empirical absorption correction multi-scan was performed using the *SADABS* (Bruker 2004) program. The crystal structures of both compounds were obtained by direct methods using SHELXD2013. The structures were refined by the full-matrix least-squares method using SHELXL2013 (Sheldrick 2008). All non-hydrogen atoms were refined using anisotropic temperature factors. The final difference Fourier maps for all compounds at this stage were critically inspected and the hydrogen atoms were located and included in the refinement, only with isotropic temperature factors. The accuracy of the crystal structures was evidenced from the final residual *R*- and *wR*- factors and other parameters including estimated standard deviations in the values of bond length and bond angles, 'data-to-parameter' ratio, etc. Details of the crystal data, data collection and refinement are given in Table 1.

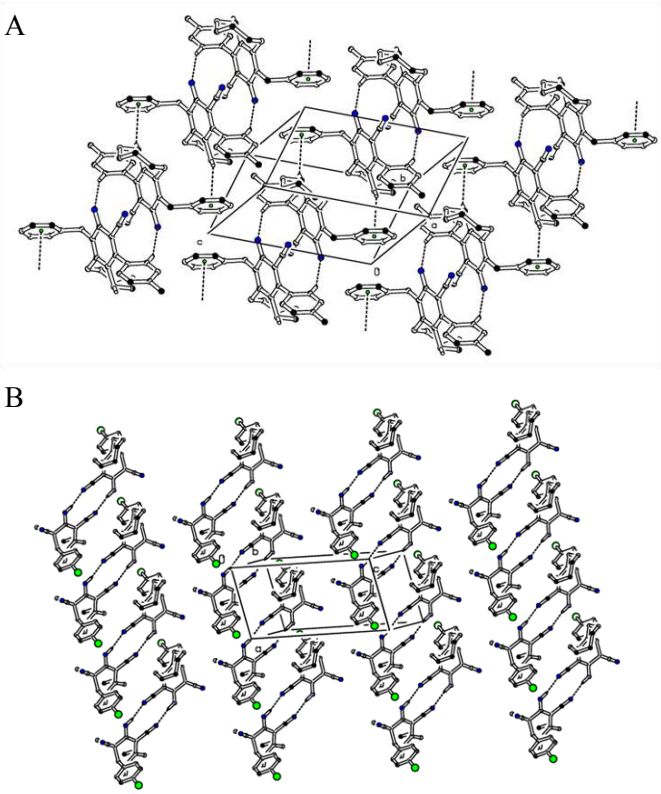

Figure 3: The inversely related molecules forms a ring motif $R_2^2(12)$ which are linked through Van der Waal's interactions. A, compound (Ia); B, compound (Ib).

Docking studies

The coordinates of enoyl acyl carrier protein (2NSD)

Table 2. Hydrogen bonds [Å and °] of compound (Ia). Symmetry transformations used to generate equivalent atoms: *(-x, - y, - z).*

D-HA	d(D-H)	...d(HA)	...d(DA)	<DHA
C1-H1-Cl1	0.98	2.54	3.087 (15)	115
N4-H4A-N1 [(i)]	0.86	2.16	3.015(2)	170

with Nad and N-acetyl-gamma-glutamyl-phosphate reductase (2NQT) were retrieved from the RCSB protein data bank (http://www.pdb.org). The target protein of 2NSD contains two monomers. Only one monomer was selected for docking analysis. The protein structures were cleaned using the whatif online server (http://swift.cmbi.ru.nl/whatif/). The protein's active site pocket was identified using 'Computed Atlas of Surface Topography' (http://sts.bioe.uic.edu/castp/). Preparation of protein and ligand input structures and the definition of the binding sites were carried out under a GRID-based procedure. A rectangular grid box was constructed over the protein with grid points 90X90X90 $Å^3$ separated by 0.375 Å under the docking procedure. The lowest energy cluster returned by AutoDock for each compound was considered and used for further analysis. Consequent runs were set up to 100 for each inhibitor. All other parameters were maintained at their default settings. All the docking result visualizations are achieved by using the 'PDBsum Generate' online server (https://www.ebi.ac.uk/pdbsum/).

Table 3. Hydrogen bonds [Å and °] of compound (Ib). Symmetry transformation used to generate equivalent atoms: *(1 - x, 1 - y, -z).*

D-HA	d(D-H)	...d(HA)	...d(DA)	<DHA
N4-H4A-N1 [(i)]	0.86	2.13	2.974(5)	169

Results

The molecular structures of compounds (Ia) and (Ib) are shown in Figure 2. The two compounds differ in the nature of the substituent at position 2 and 4 of the phenyl ring. This simple change in the structures results in the change of structure types. In both compounds, the cyclohexane ring adopts a boat conformation with puckering parameters Q = 0.445(17) Å, Θ = 65.5(2)° and Φ = 39.4(2)° in compound (Ia); Q = 0.406 (4) Å, Θ = 115.6(6)° and Φ = 210.4(7)° in compound (Ib). The cyclooctane ring adopts a twisted chair-chair conformation in compounds (Ia) and (Ib) as found in related structures (Fun *et al.* 2010, Suresh *et al.* 2007). The triple-bond characters of C13 ≡ N1, C14 ≡ N2 and C15 ≡ N3 [1.138(2) Å , 1.131(2) Å, 1.129(2) Å in compound (Ia) and 1.137(5) Å , 1.126(5) Å, 1.127(5) Å in compound (Ib), respectively] as well as the bond angles of C4-C13≡N1, C2-C14≡N2 and C2-C15≡N3 [179.2(2)° , 178.5(2)°, 178.2(2)° in compound (Ia) and

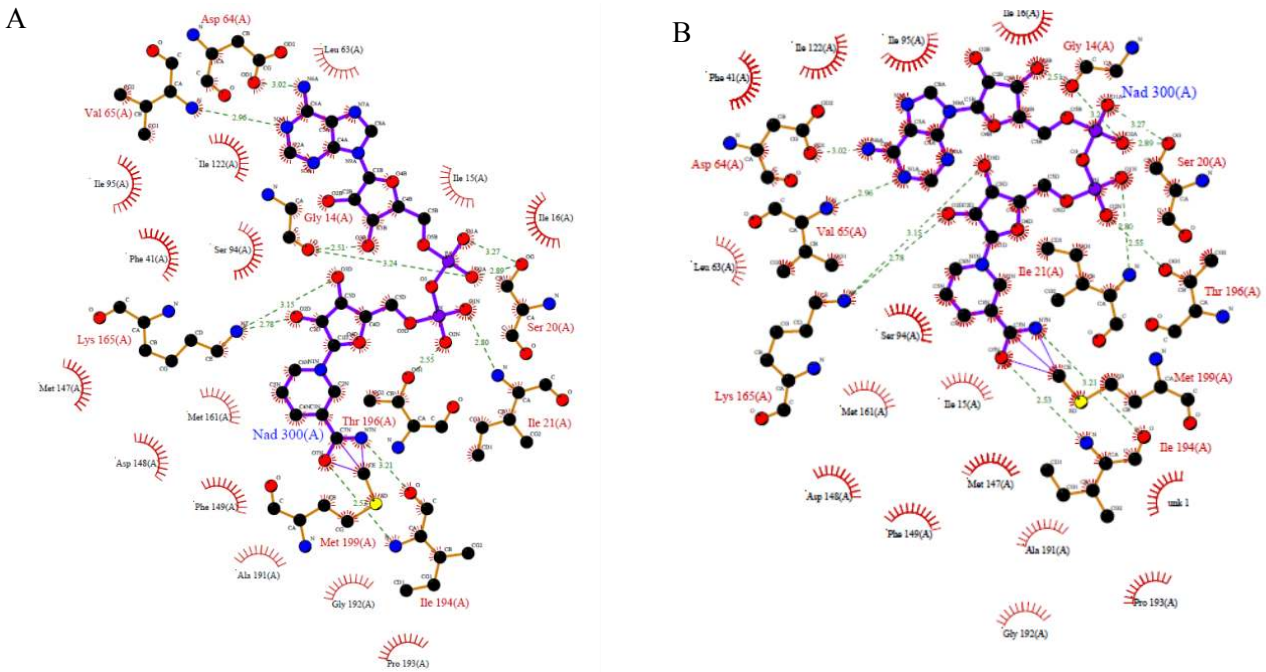

Figure 4: Enoyl acyl carrier protein with Nad interactions for compound (Ia) (A) and (Ib) (B).

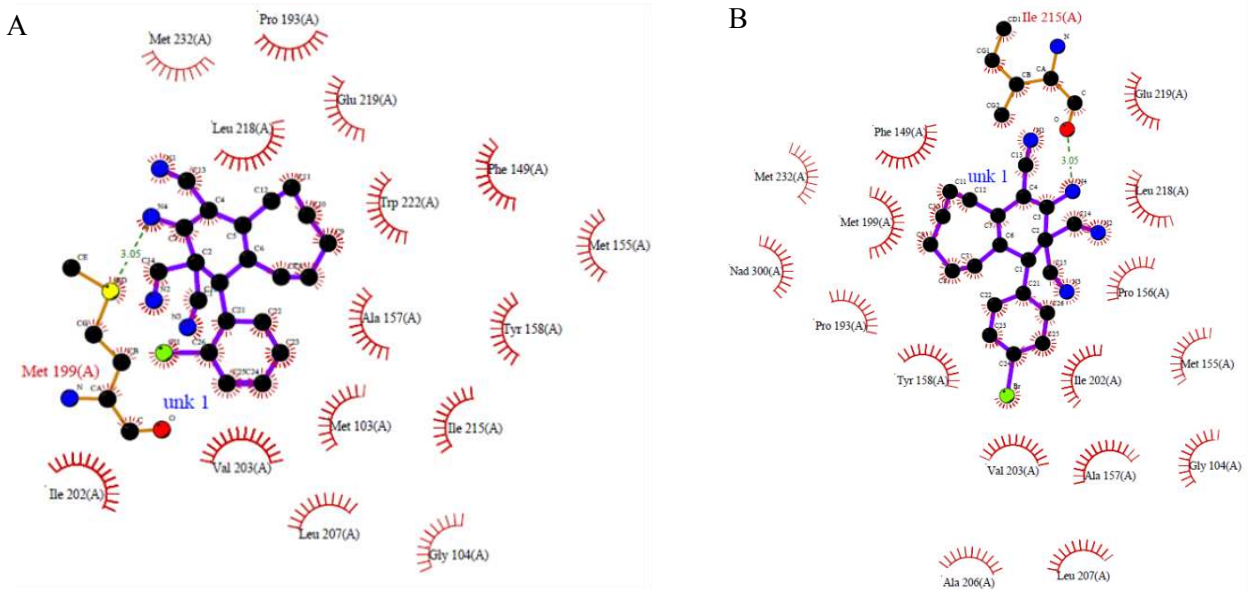

Figure 5. Interactions of compound (Ia) (A) and (Ib) (B) with protein.

179.2(5)°, 178.9(4)°, 178.7(4)° in compound (Ib), respectively] in both compounds define the linearity of the cyano carbonitrile compounds. The phenyl substituent of the cycloheaxne ring at C1 has a negative synclinal conformation in compound (Ia) and negative anticlinal conformation in compound (Ib), as evidenced by the C2–C1–C21–C22 [-83.67° in compound (Ia) and -112.5° in compound (Ib) torsion angles]. The aryl ring in the structure (Ib) is not coplanar with the mean plane of the cyclohexane ring. This lack of coplanarity is caused by non-bonded interactions between one of the ortho H atoms in the aryl ring and a hydrogen atom at the C1 position of the cyclohexane ring. Steric repulsions are reduced by the expansion of the C1–C21– C26 angle in structure (Ib).

Crystal packing

Inter molecular hydrogen bond geometry of compound (Ia) and compound (Ib) are listed in Table 2. In the crystal structure of compound (Ia) the N4 atom of the cyclohexane ring is involved in the intermolecular interaction N4—H4A···N1$^{(i)}$ with the N1 atom (Table 2). This forms a $R_2^2(12)$ ring motif (Bernstein *et al.* 1995) [symmetry code: (i) (- x, - y, – z)]. These adjacent ring motifs are linked together via Van der Waal's interactions as shown in Figure 3.

In the crystal structure of the compound (Ib) the intermolecular interaction N4—H4A···N1$^{(i)}$ (with the N1 atom) (Table 2) forms a R_2^2 ring motif (12) (Bernstein *et al.* 1995) [symmetry code: (i) (2 - x, 1 - y, – z)]. These adjacent ring motifs are linked together by van der Waal's interactions, as shown in Figure 3.

The N—N distance is longer in compound (Ia) [3.015(2) Å] compared to (Ib) [2.974(5) Å] and the N—H···N angle in compounds (Ia) and (Ib) are 169° and 170°, respectively. This shows that the 4-bromine substituent forms a stronger hydrogen bond than the 2-cholorine substituent.

Docking analysis

The target protein structure of 2NSD with Nad was docked with the synthesized compounds using AutoDock4v2 (Goodsell 1998). The synthesized compounds were found to display good binding affinity to the receptor with minimum binding energy equal to -9.47 and -10.70 for (Ia) and (Ib), respectively. The Nad interactions of the compounds are shown in Figure 4.

In compound (Ia), the nitrogen atom of the benzo ring is hydrogen bonded to MET^{199}, one of the catalytic residues in the InhA active site, as shown in Figure 4. Rozwarski *et al.* (1999) have shown that hydrophobic aminoacids of the loop are important for proper substrate binding into the cavity. Interestingly, the last few carbon atoms of the fatty acid interact with the hydrophobic amino acids Ala^{198}, Met^{199}, and Ile^{202}. Our (Ia) inhibitor is able to directly interact with one of these residues (Met^{199}), leads to a defined loop structure and has hydrophobic interactions to the important loop residues of InhA, resulting in a slow tight binding inhibition. In our (Ib) compound, the nitrogen atom of the benzo ring is hydrogen bonded to Ile^{215}, one of the catalytic residues in the InhA active site and has hydrophobic interactions with Ala^{198} and Met^{199}, as shown in Figure 5.

The target protein structure of 2NQT was docked with the synthesized compounds using AutoDock4v2 (Goodsell, 1998). The synthesized compounds were found to display good binding affinity to

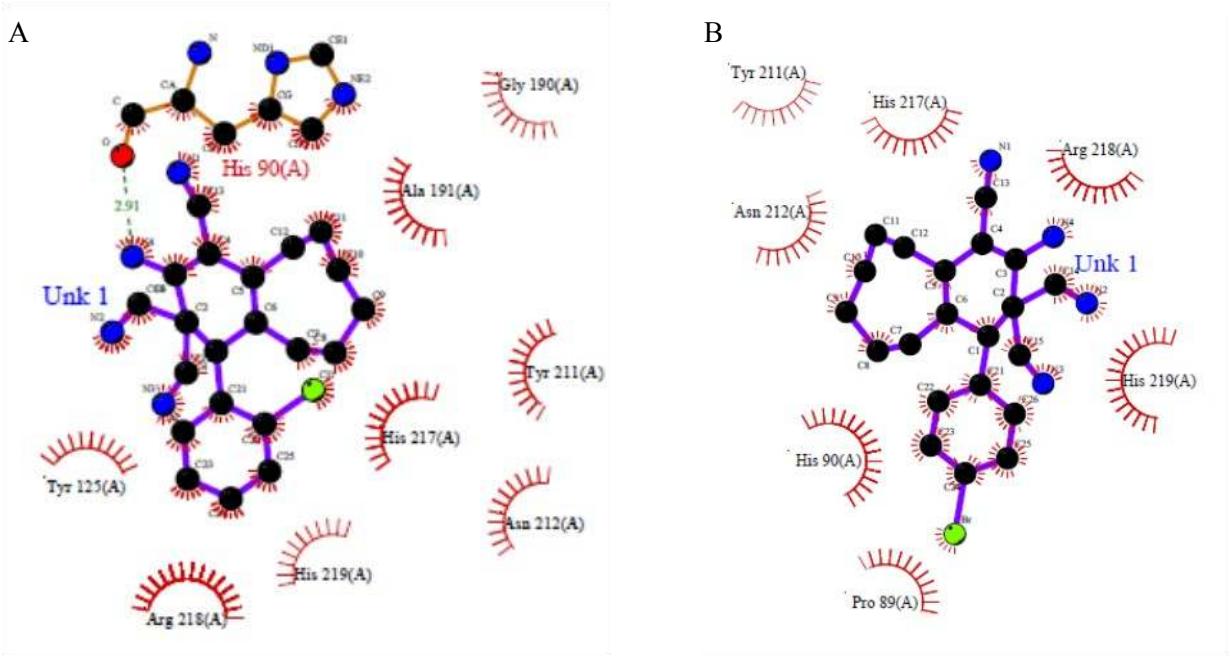

Figure 6. Interactions of compounds (Ia) (A) and (Ib) (B) with protein.

the receptor with minimum binding energy equal to -6.25 and -7.18, for compounds (Ia) and (Ib), respectively.

In compound (Ia), the nitrogen atom of the benzo ring is hydrogen bonded to His^{90}, where as in compound (Ib), the ligand has hydrophobic interactions with the protein (Figure 6).

Conclusion

Our goal is to propose new TB inhibitors. In this direction, we synthesized two novel compounds of benzoannulene derivatives. The compounds were docked with the enoyl-aceyl carrier protein and the N-acetyl-gamma-glutamyl-phosphate reductase. Their free binding energies were evaluated. Both compounds showed good binding affinity, which is indicative of stable, energetically viable complexes. Hence, our synthesized ligands bear promising *in silico* anti-tubercular activities. From the docking analysis of the two compounds with both protein receptors, it was found that (Ib) shows better binding with the receptors, as compared to (Ia).

Authors' Contribution

Authors 1 and 2 were involved in the data collection, crystallography and docking work. Authors 3 and 4 were involved in the synthesis and crystal growth of the title compounds. First author is the second author's student and third author is the fourth author's student.

Supplementary Material

Crystallographic data (excluding structure factors) for the structures of **(**Ia) and (Ib) reported in this paper have been deposited with the Cambridge Crystallographic data Centre as supplementary publication CCDC 1436956 & CCDC 1436957. Copies of the data can be obtained, free of charge, on application to, CCDC, 12 Union Road, Cambridge, and CB2 1 EZ UK; Fax: 044-1223-336033; Email: deposit@ccdc.cam.uk or at: http://www.ccdc.cam.ac.uk/

Acknowledgements

JS and RAN thank the management of The Madura College (Autonomous), Madurai for their encouragement and support. RRK thanks the University Grants Commission, New Delhi, for funds through Major Research Project F. No. 42-242/2013 (SR). SM thanks the university grants commission, New Delhi for the fellowship under the UGC-BSR-JRF meritorious scheme.

Conflicts of interest

The authors have no conflicts of interest.

References

Bernstein J, Lott WA, Steinberg BA & Yale HL 1952 Chemotherapy of experimental tuberculosis. *Am Rev Tuberc* **65** 357-374

Bradford WZ & Daley CL 1998 Multiple drug-resistant tuberculosis. *Infect Dis Clin North Am* **12** 157 -172

Bruker 2004 APEX2 and SAINT. Bruker AXS Inc., Madison, Wisconsin, USA.

Cybis J & Davis RH 1975 Organization and control in the arginine biosynthetic pathway of Neurospora. *J Bacteriol* **123** 196-202

Dessen A, Quémard A, Blanchard JS, Jacobs WR Jr & Sacchettini JC 1995 Crystal structure and function of the isoniazid target of Mycobacterium tuberculosis. *Science* **267** 1638-1641

Fun HK, Yeap CS, Ragavan RV, Vijayakumar V & Sarveswari S 2010 4,5,6,7,8,9-Hexahydro-2H-cyclo-octa[c]pyrazol-1-ium-3-olate. *Acta Crystallogr Sect E Struct Rep Online* **66** o3019

Goodsell DS, Morris GM & Olson AJ 1998 Automated docking of flexible ligands: Applications of autodock. *J Mol Recog* **9** 1-5

Koci J, Klimesova V, Waisser K, Kaustova J,Dahse H-M & Mollmann U 2002 Heterocyclic benzazole derivatives with antimycobacterial in vitro activity. *Bioorg Med Chem Lett* **12** 3275-3278

Nagalakshmi RA, Suresh J, Maharani S & Ranjith Kumar R 2014 Crystal structure and molecular docking studies of octahydrocycloocta[b]pyridine-3-carbonitriles as potential inhibitors against Mycobacterium tuberculosis. *J Mol Biochem* **3** 77-84

Rozwarski DA, Grant GA, Barton DH, Jacobs WR Jr & Sacchettini JC 1998 Modification of the NADH of the isoniazid target (InhA) from Mycobacterium tuberculosis. *Science* **279** 98-102

Rozwarski DA, Vilchèze C, Sugantino M, Bittman R & Sacchettini JC 1999 Crystal structure of the Mycobacterium tuberculosis enoyl-ACP reductase, InhA, in complex with NAD+ and a C16 fatty acyl substrate. *J Biol Chem* **274** 15582-15589

Sanna P, Carta A & Nikookar ME 2000 Synthesis and antitubercular activity of 3-aryl substituted-2-[1H(2H) benzotriazol-1(2)-yl]acrylonitriles. *Eur J Med Chem* **35** 535-543

Schluger NW, 2005 The pathogenesis of tuberculosis: the first one hundred (and twenty-three) years. *Am J Respir Cell Mol Biol* **32** 251-256

Sheldrick GM 2008 A short history of *SHELX*. *Acta Cryst* A **64** 112-122

Smith I 2003 Mycobacterium tuberculosis pathogenesis and molecular determinants of virulence. *Clin Microbiol Rev* **16** 463-496

Spek AL 2009 Structure validation in chemicalcrystallography. *Acta Cryst* D **65** 148-155

Suresh J, Vishnu Priya R, Sivakumar S & Ranjith Kumar R 2012 Spectral analysis and crystal structure of two substituted spiro acenaphthene structures. *J Mol Biochem* **1** 183-188

Tiruviluamala P & Reichman LB 2002 Tuberculosis. *Annu Rev Public Health* **23** 403-426

Vishnupriya R, Kowsalyadevi AVKM, Suresh J, Maharani S & Kumar RR 2014 Crystal structure and docking studies of hexahydrocycloocta[b]pyridine-3-carbonitriles. *J Mol Biochem* **3** 50-57